Radiaiton Belts

Yuri Shprits[1,2]

[1]Institute of Geophysics and Planetary Physics, UCLA

[2]Department of Earth and Planetary Sciences, UCLA

Acknowledgements: Alexander Ukhorskiy, Dmitri Subbotin, Ksenia Orlova, Marianne Daae

Talk outline

1. Introduction: Discovery of the Radiation Belts. Kinematics of radiation belt electrons and the quiet time structure of the radiation belts
2. Radiation acceleration mechanims
3. Radiation belt particle losses
4. 3D simulations of the Radiation Belts using Versatile Electron Radiation Belt code

First discovery of space age

January 31, 1958: The US Explorer 1 satellite is launched into orbit with a Geiger counter on board. James Van Allen discovered that space is radioactive

~250 satellites; Supporting $25 billion/ year industry ;Replacement cost: $75 billion;

Space weather–induced effects on an Earth-orbiting spacecraft:

(A) Single-event upsets (SEUs) due to energetic ions;

(B) Deep-dielectric charging due to relativistic electrons;

(C) Surface charging due to moderate-energy electrons.

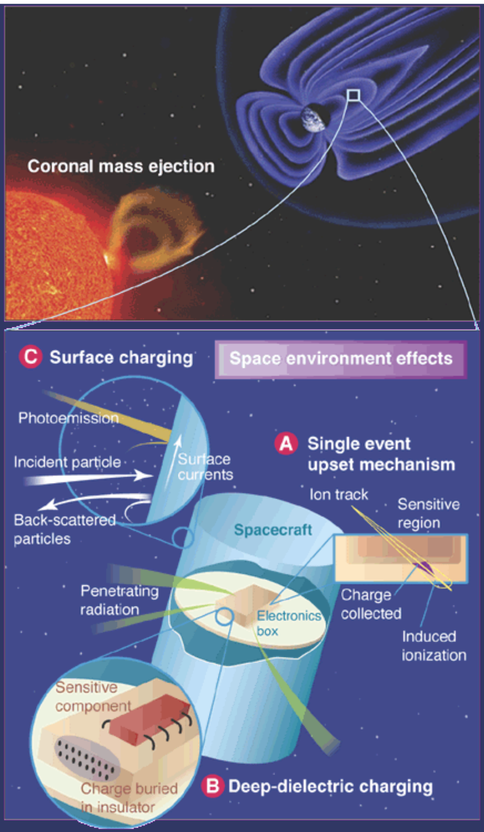

Baker et al., 2002;
Odenwald., 2006]

Two-Zone Structure

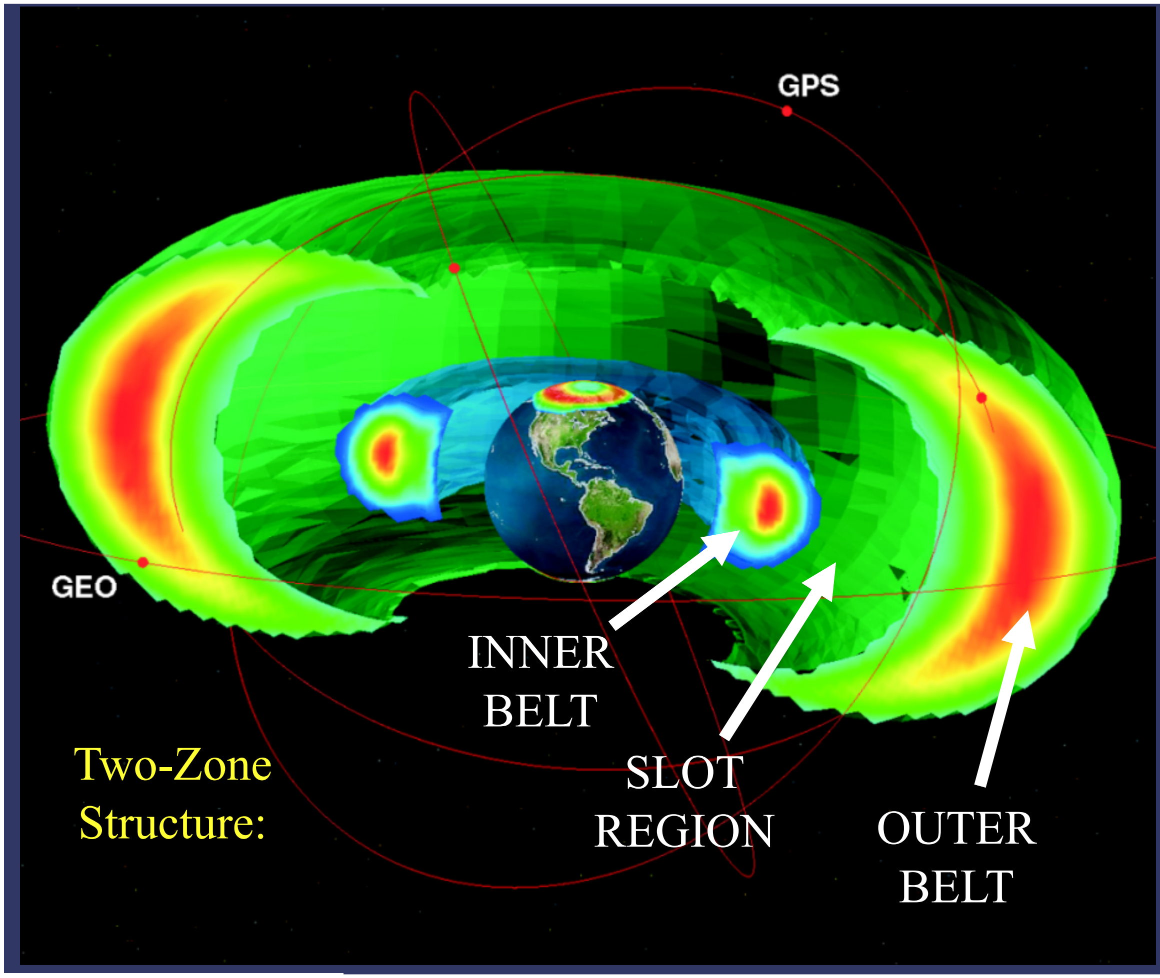

- Radiation belts
  - energies >100 keV
  - two-zone structure
- Inner belt: fairly stable
- Outer belt: can change on the time scale of an hour.

Charged Particle Motion

E = 0, **B** = const

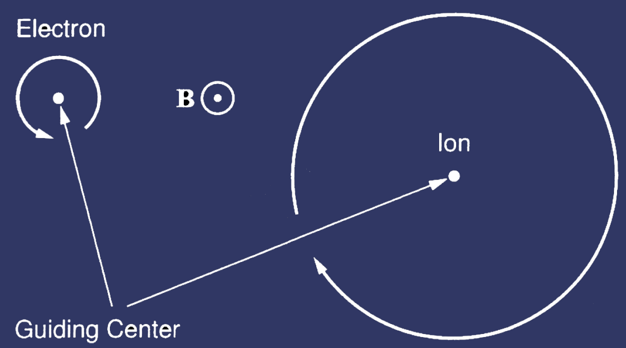

Uniform rotation at cyclotron frequency:

E = 0, **B** ≠ const

$\rho|\nabla B| \ll B$

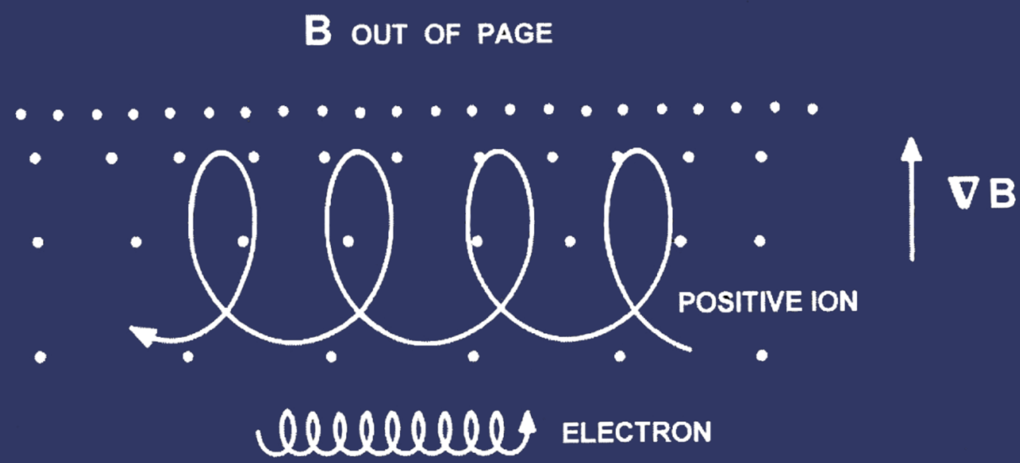

Variation of the magnetic field intensity causes guiding center drift perpendicular to the field and its gradient:

Bounce Motion in the Magnetic Bottle

$$\mu = \frac{p_\perp^2}{2mB} = \frac{p^2}{2mB_m} \qquad F_\parallel = \frac{1}{\gamma}\mu \cdot \nabla B$$

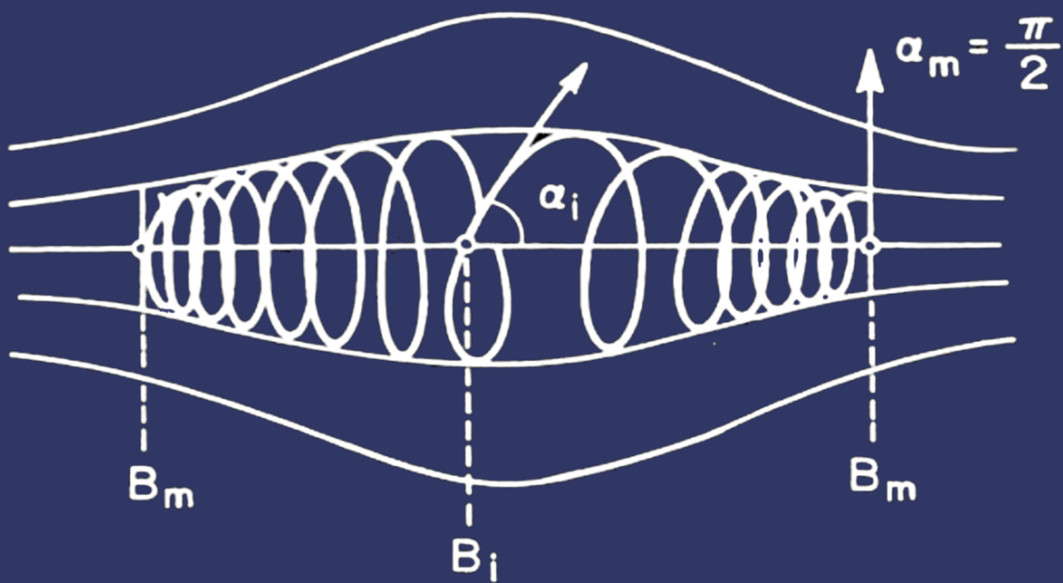

Charged particles undergo bounce motion in the magnetic botel.

Pitch-angle of the particle changes from the maximum value on the equator to 90 ° in the mirror point.

Courtesy of A. Ukhorskiy

Bounce Motion

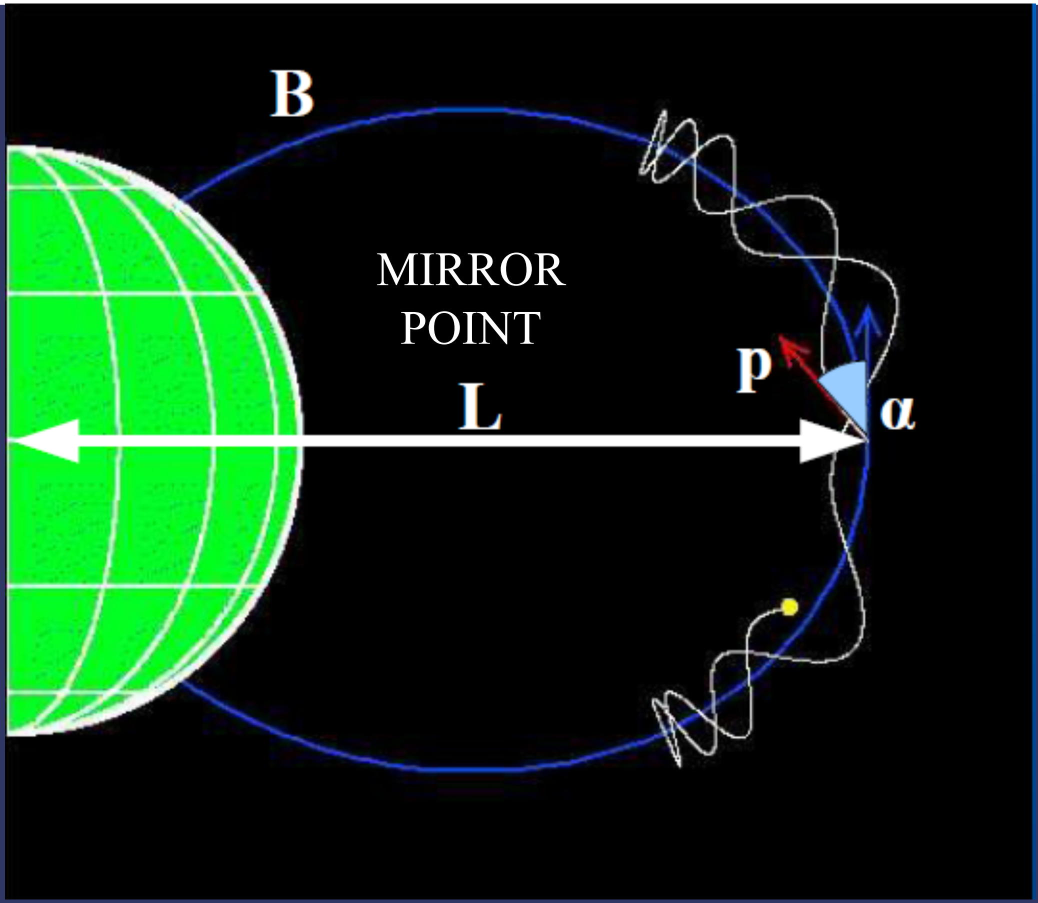

Pitch-angle – the angle between the magnetic field and particle's velocity.

90˚ pitch-angle particles will stay in the equatorial plane

Small pitch-angle particles will be lost to the atmosphere.

Trajectories of the Radiation Belt Particles

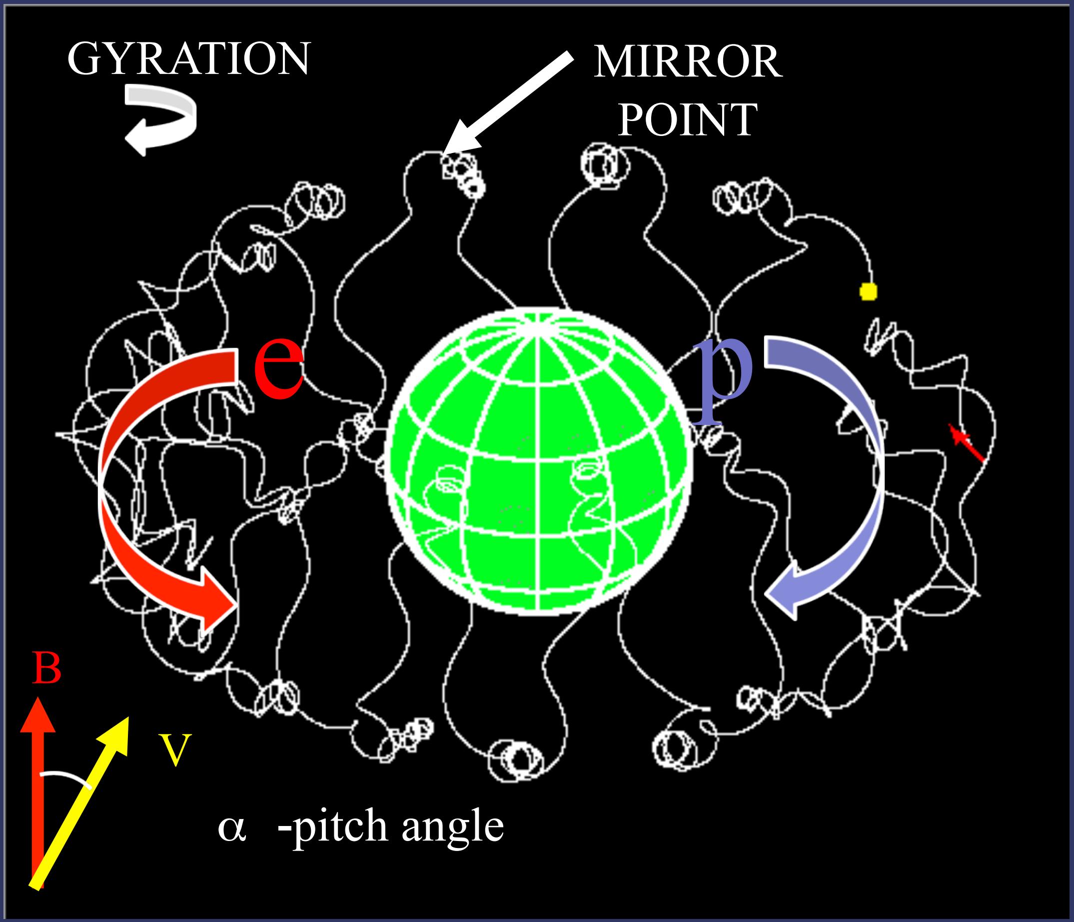

Gyro motion around the field line,

Bounce motion between the mirror points

Slow drift around the Earth.

Each type of periodic motion can be associated with an adiabatic invariant.

Simulations of the drift of 1 MeV electron, $m=20m_e$

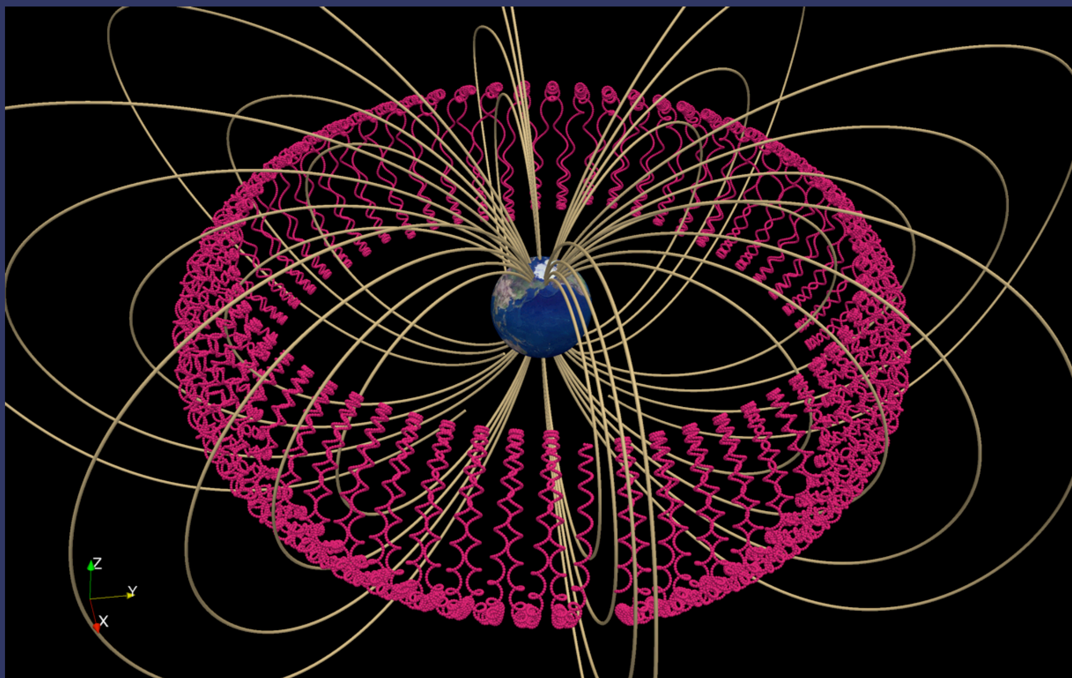

Gyro motion around the field line,

Bounce motion between the mirror points

Slow drift around the Earth.

Each type of periodic motion can be associated with an adiabatic invariant.

Courtesy of Sasha Ukhorskiy

Simulations of the drift of 1 MeV electron

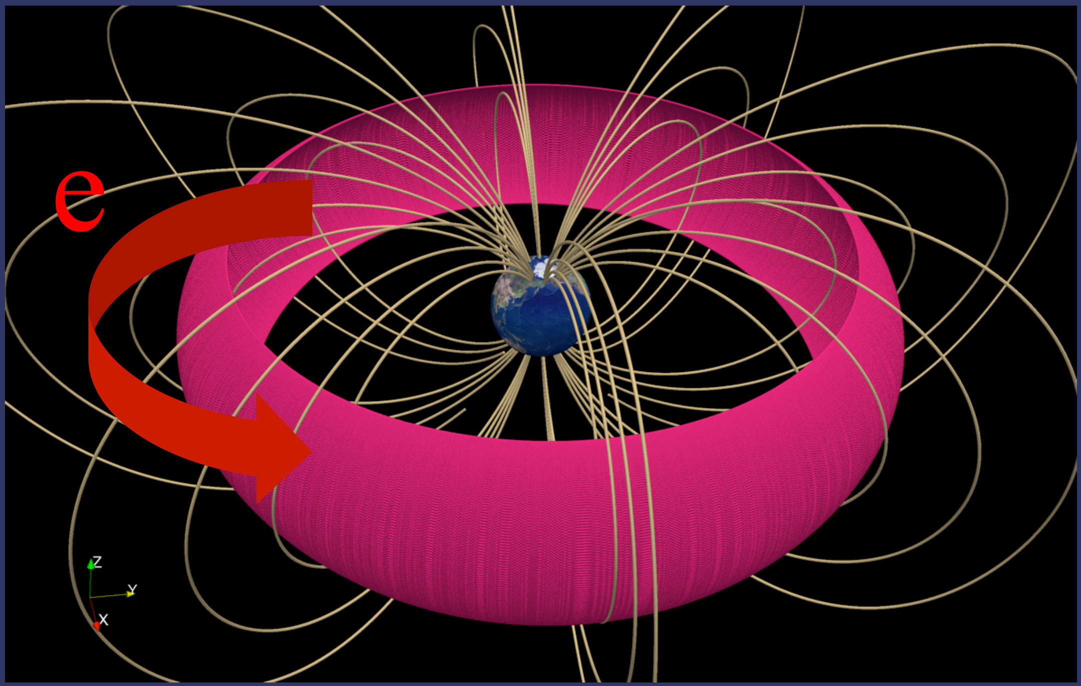

Gyro motion around the field line,

Bounce motion between the mirror points

Slow drift around the Earth.

Each type of periodic motion can be associated with an adiabatic invariant.

Courtesy of Sasha Ukhorskiy

Adiabatic invariants

$$\mu = \frac{p_\perp^2}{2m_0 B}$$

$$J = \oint p_\parallel ds$$

$$\Phi = \int B dS$$

$$L^* = \frac{2\pi M}{\Phi R_E}$$

$$J(E,\alpha) = f(\mu, J, L^*) / p^2$$

$$\frac{\partial f}{\partial t} = \sum_{m,n=1}^{3} \frac{\partial}{\partial J_m} D_{J_m J_n} \frac{\partial}{\partial J_n} f\,;$$

Fokker-Planck equation

Radial diffusion   Pitch-angle diffusion   Energy diffusion

$$\frac{\partial f}{\partial t} = \boxed{L^2 \frac{\partial}{\partial L} L^{-2} D_{LL} \frac{\partial f}{\partial L}} + \boxed{\frac{1}{T(y)y} \frac{\partial}{\partial y} T(y) y D_{yy} \frac{\partial f}{\partial y}} + \frac{1}{p^2} \frac{\partial}{\partial p} p^2 D_{pp} \frac{\partial f}{\partial p}$$

$$y = \sin(\alpha)$$

Inward radial diffusion can redistribute fluxes and provide energization or loss

Pitch angle scattering produces loss of electrons to the atmosphere

Energy diffusion provides local source of particles

Dominant Acceleration and Loss Mechanisms during Quiet Times

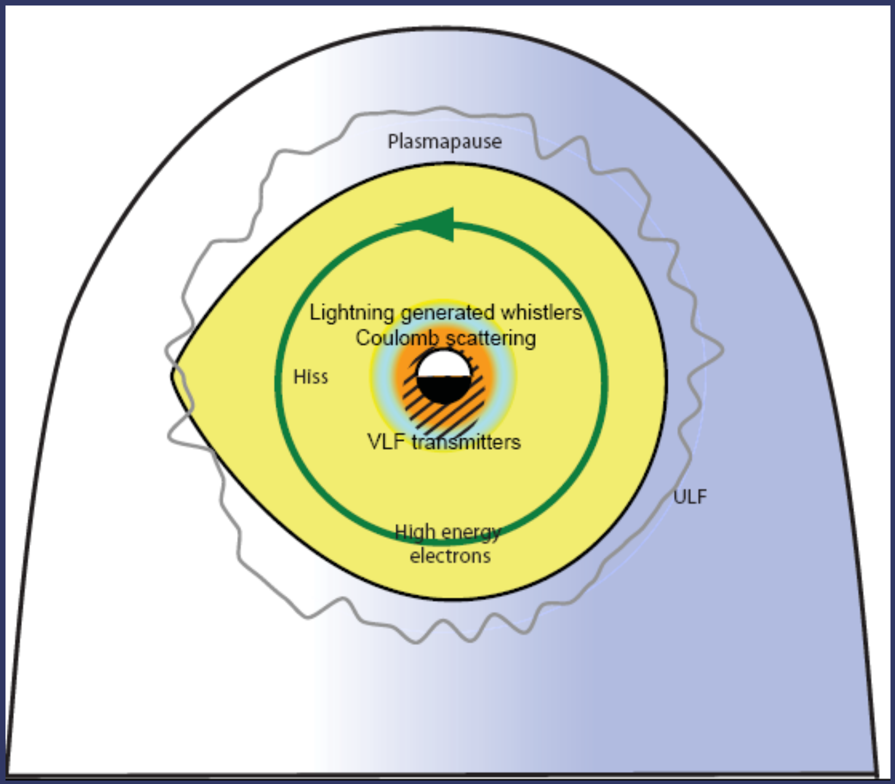

Inward radial diffusion driven by ULF waves.

Plasmaspheric Hiss is a dominant scattering mechanism at L>3 .

Coulomb collisions, lightening generated whistlers, anthropogenic VLF zone.

Shprits et al, 2009

Radial Diffusion

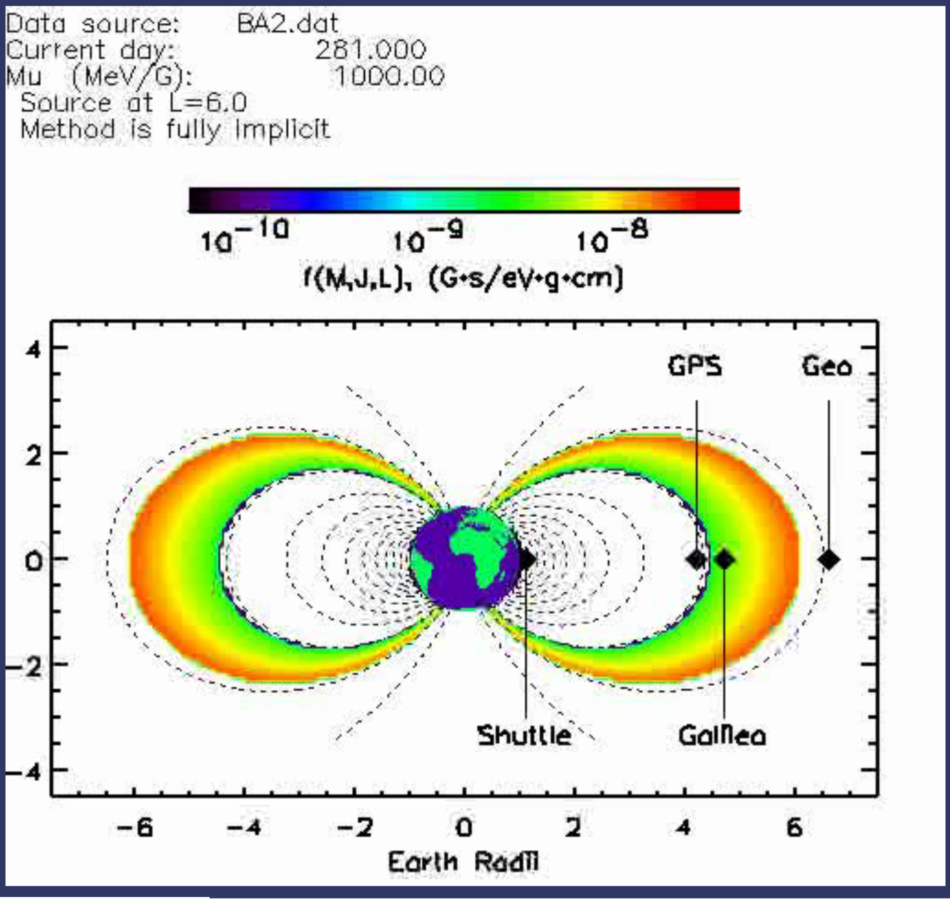

Interactions with ULF waves causes random radial displacements that can result in the radial diffusion.

Particles that are diffused into the inner region of strong magnetic field will gain energy.

Courtesy of Richard Horne

Theoretical flux profiles at fixed energy

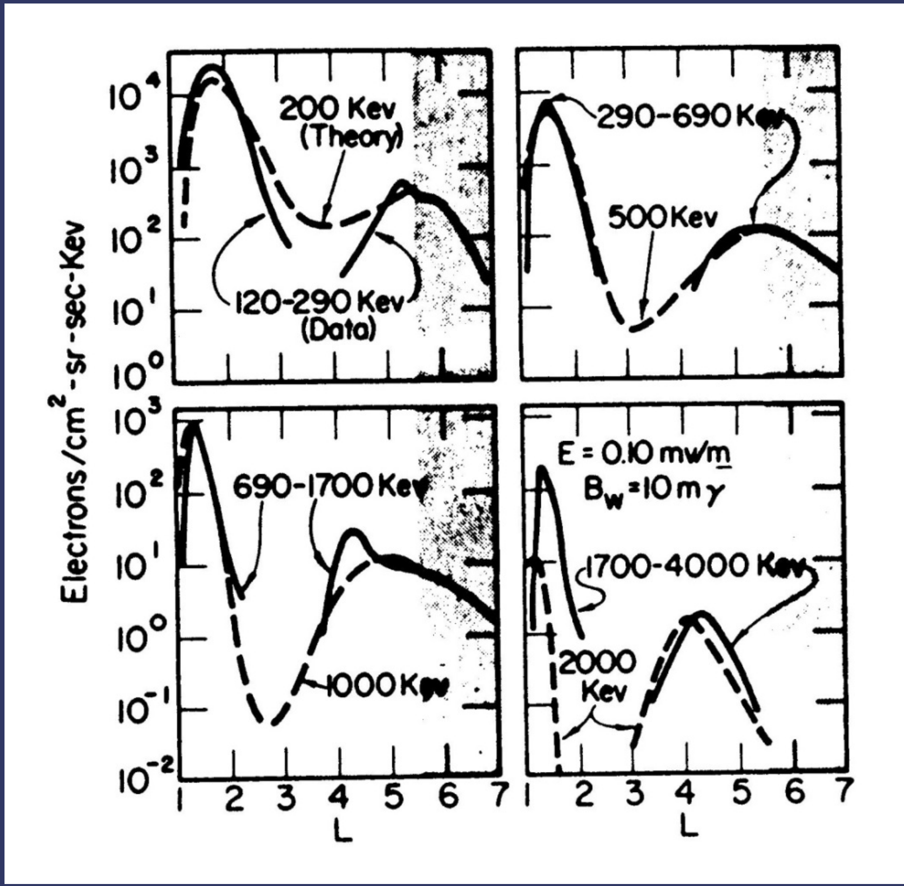

$$\frac{\partial f}{\partial t} = L^2 \frac{\partial}{\partial L}\left[D_{LL} L^{-2} \frac{\partial f}{\partial L} \right] - \frac{f}{\tau_{effective}}$$

Electron profiles obtained from the modeling of the quiet time inward diffusion

Theoretical profiles of fluxes at constant energy agree with quiet time observations.

Lyons and Thorne, 1972

Dynamical Variability of the Radiation Belt Electrons

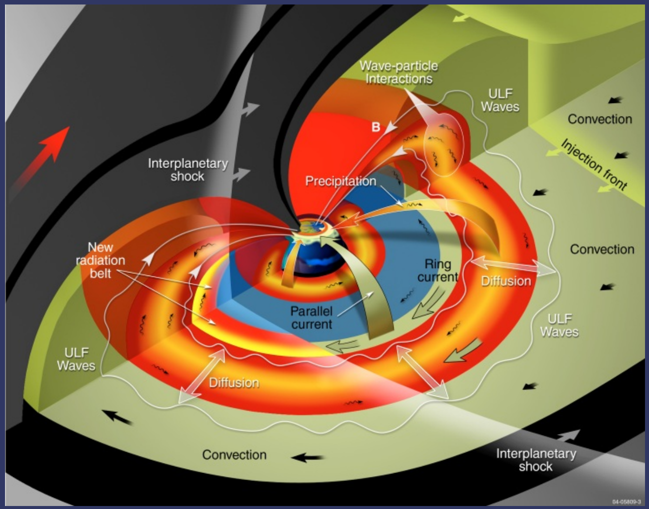

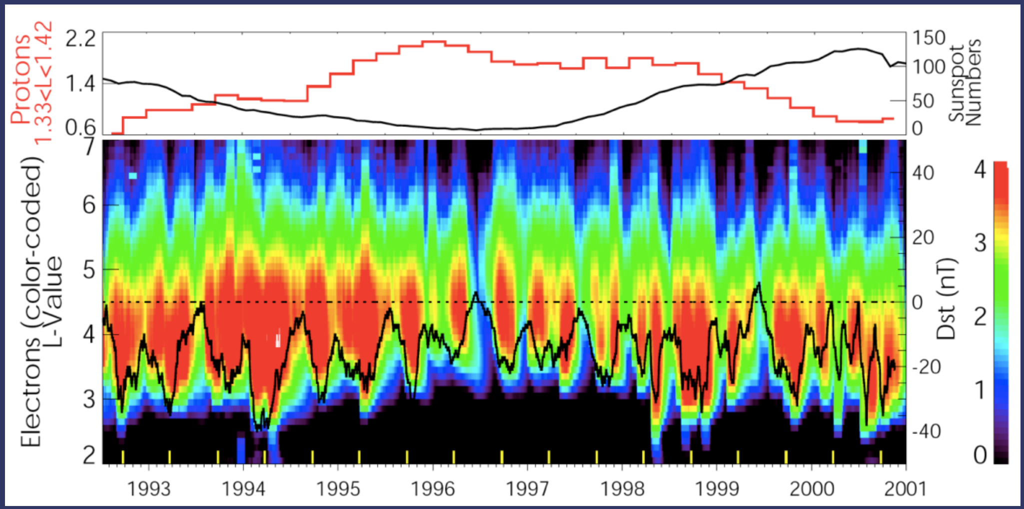

Creation and variation of radiation populations are produced by a complicated interplay of multiple processes. A broad range of coordinated measurements is needed to sort them out. How processes interact with each other under varying conditions to generate real space environments is unknown. Profound mysteries remain because existing observations are insufficient to resolve the system science.

Competition Between Acceleration and Loss

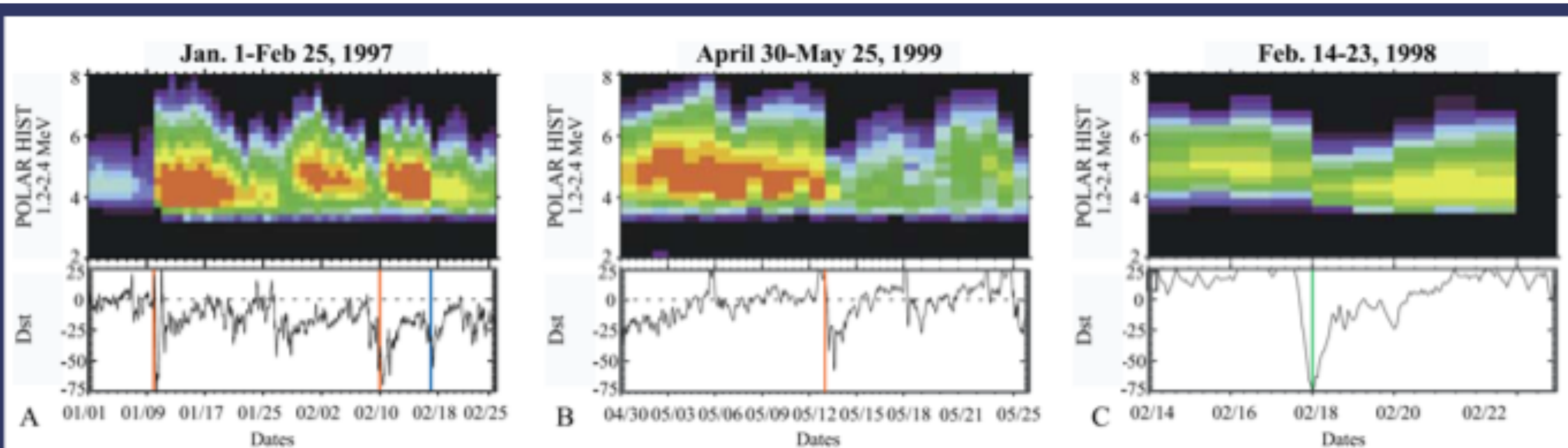

(1) Cause dramatic radiation belt enhancement;
(2) Deplete radiation belt fluxes;
(3) Cause no substantial effect of flux distributions;

How to Differentiate Between Diffusion from the Outer Source and Local Acceleration processes

(A) Phase space density increase caused by radial

diffusion from an external source.

(B) Phase space density increases predicted by local internal source acceleration mechanisms.

L* is approximately the distance from the Earth measured in Earth radii

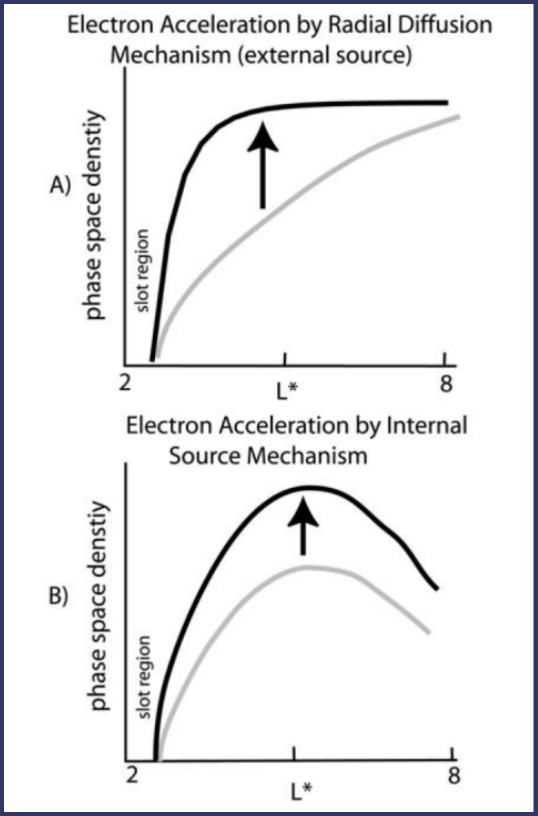

Observations of the Radial Profile of Phase Space Density

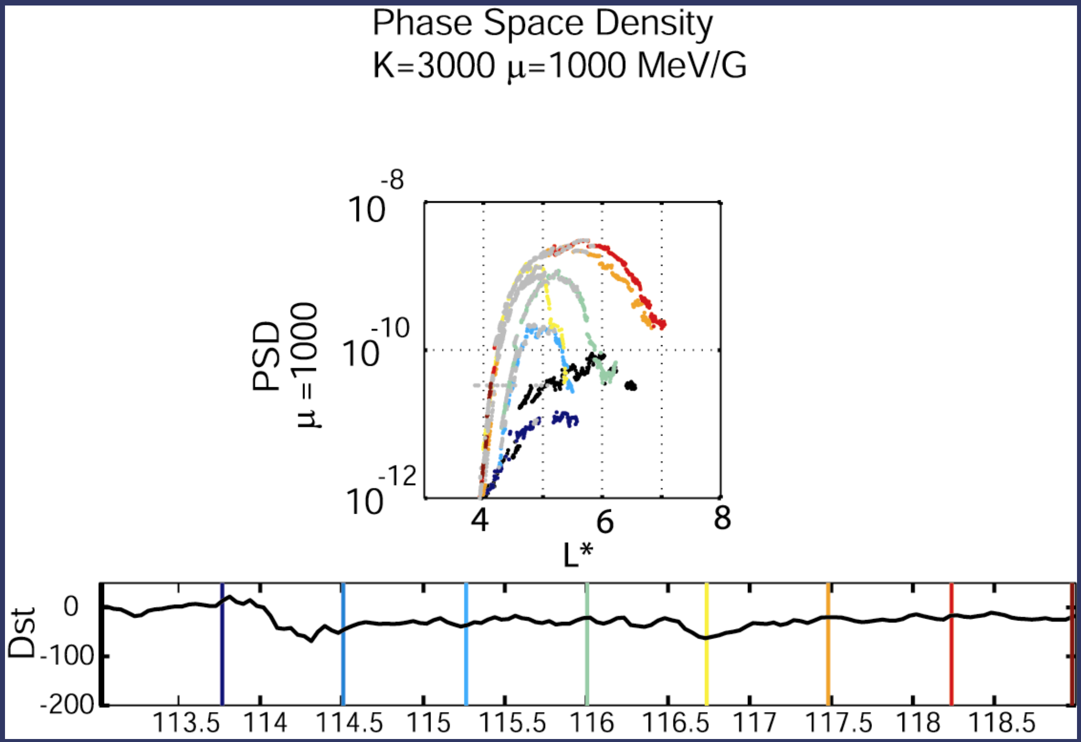

Evidence of the presence of the local acceleration source

Building up peaks are consistent with the local acceleration source produced by resonant interactions with whistler mode chorus waves.

[Green and Kivelson, 2004]

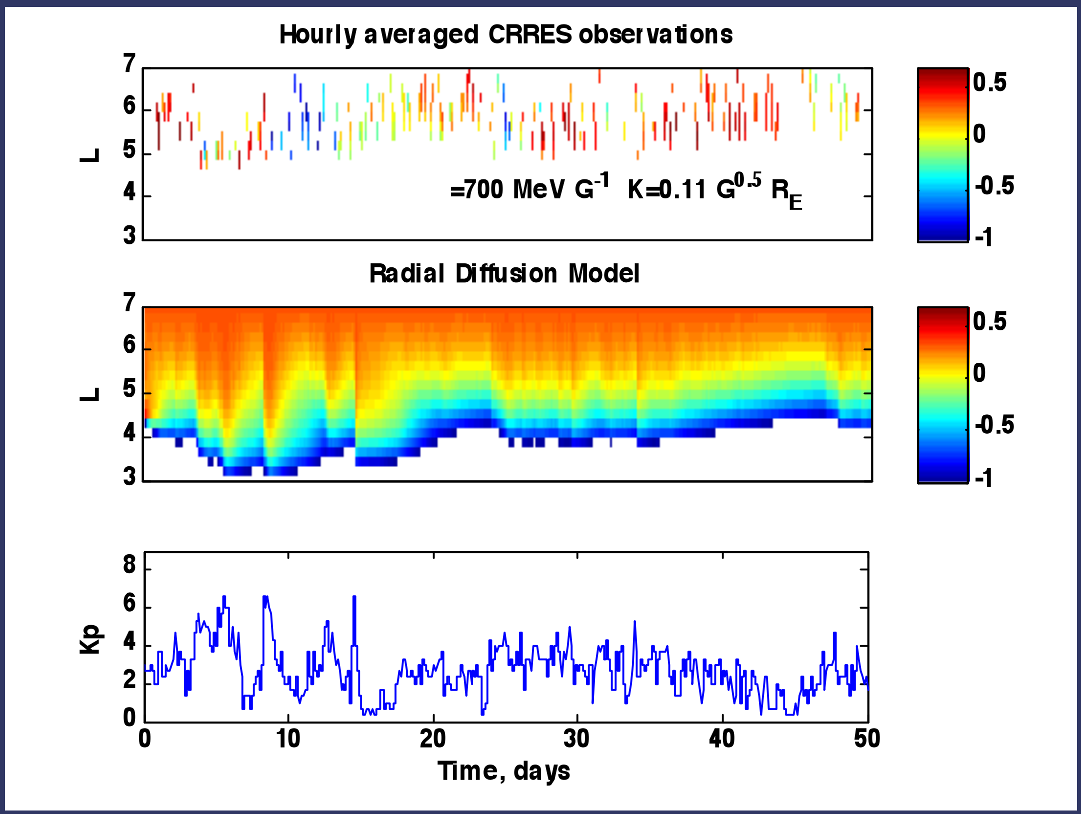

- Observations are sparse

- Model is continuous but may be missing essential physics.

Data Assimialiton with Kalman Filter

Assume initial state and data and model errors

Make a prediction of the state of the system and error covariance matrix, using model dynamics

$$w_k^f = \Psi_{k-1} w_{k-1}^f$$

Compute Kalman gain and innovation vector

Update state vector using innovation vector

$$w_k^a = w_k^f + Kd$$

Compute updated error covariance matrix

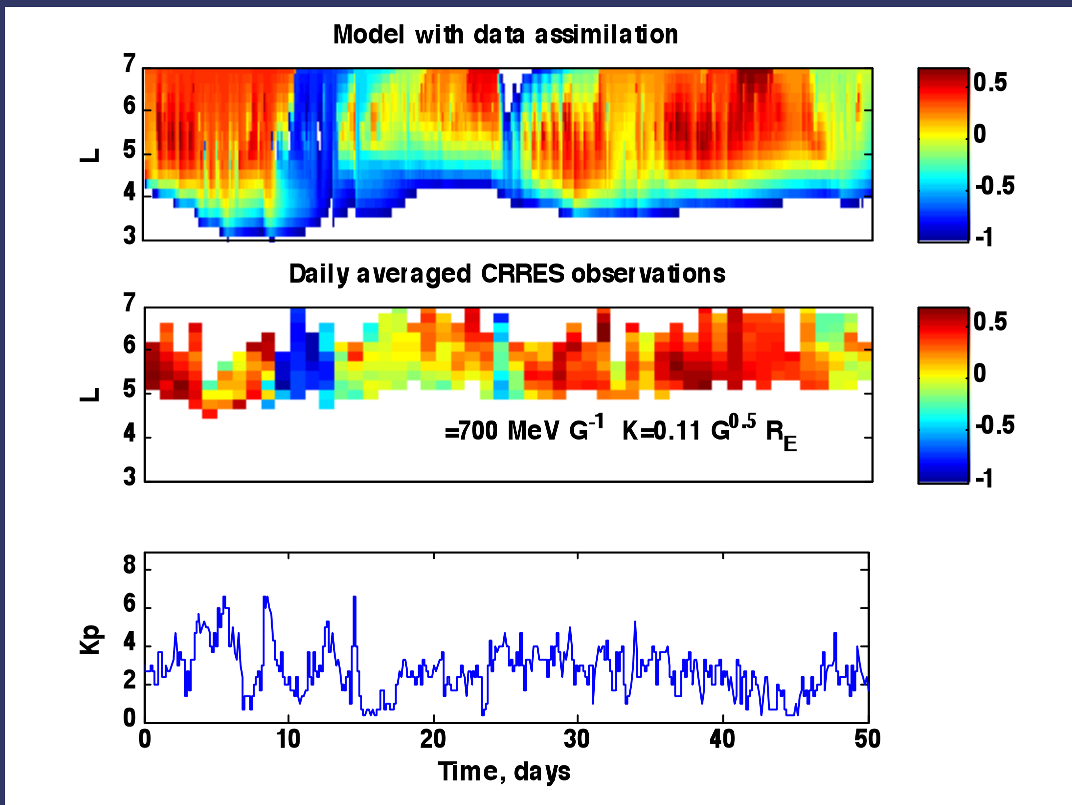

Data assimilation can fill in spatio-temporal gaps.

Data assimilation is consitstant with daily average values but allows to minimize errors and can be used with multiple spacecraft

Multi Point Observations

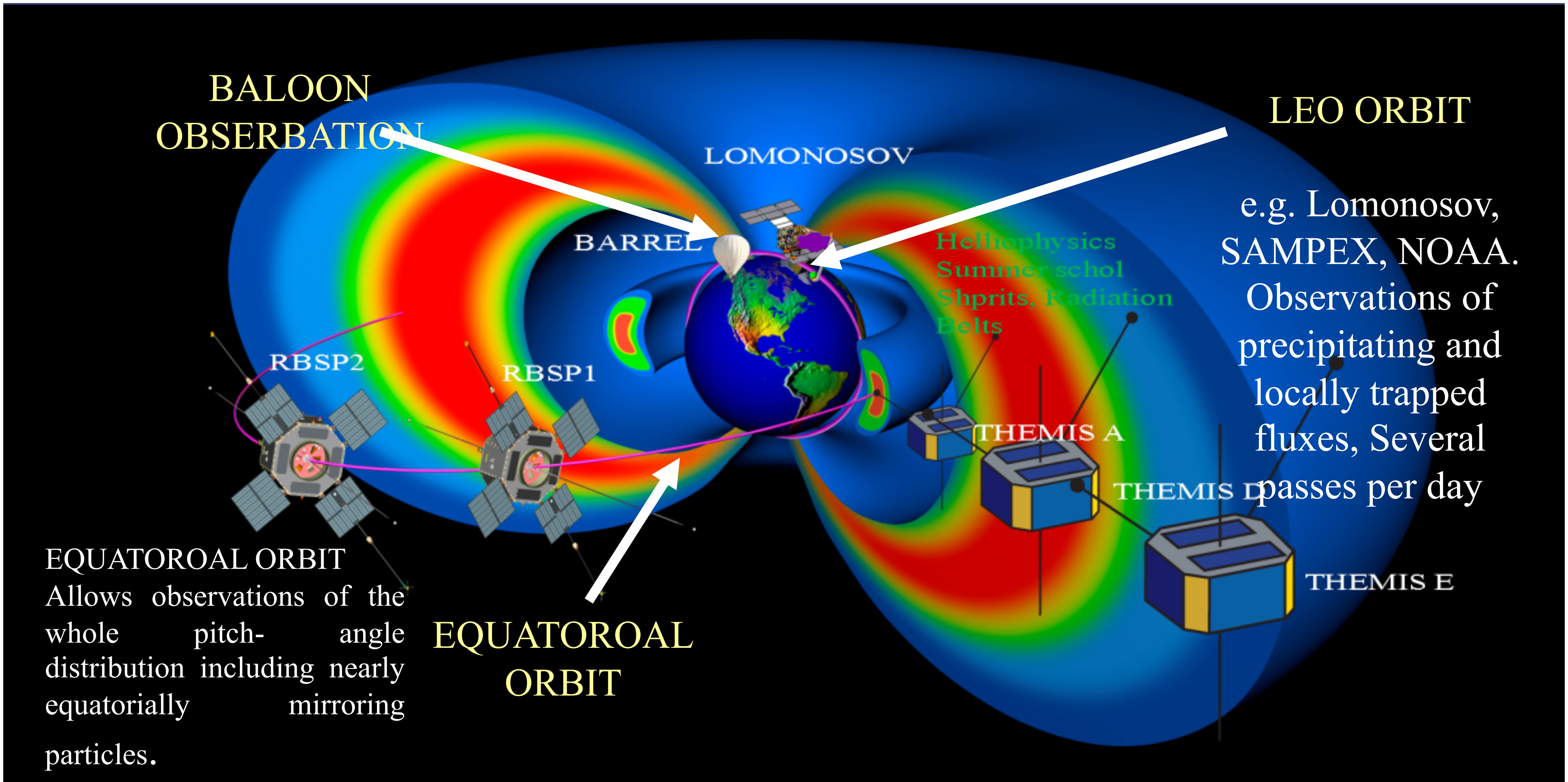

e.g. Lomonosov, SAMPEX, NOAA. Observations of precipitating and locally trapped fluxes, Several passes per day

EQUATOROAL ORBIT
Allows observations of the whole pitch- angle distribution including nearly equatorially mirroring particles.

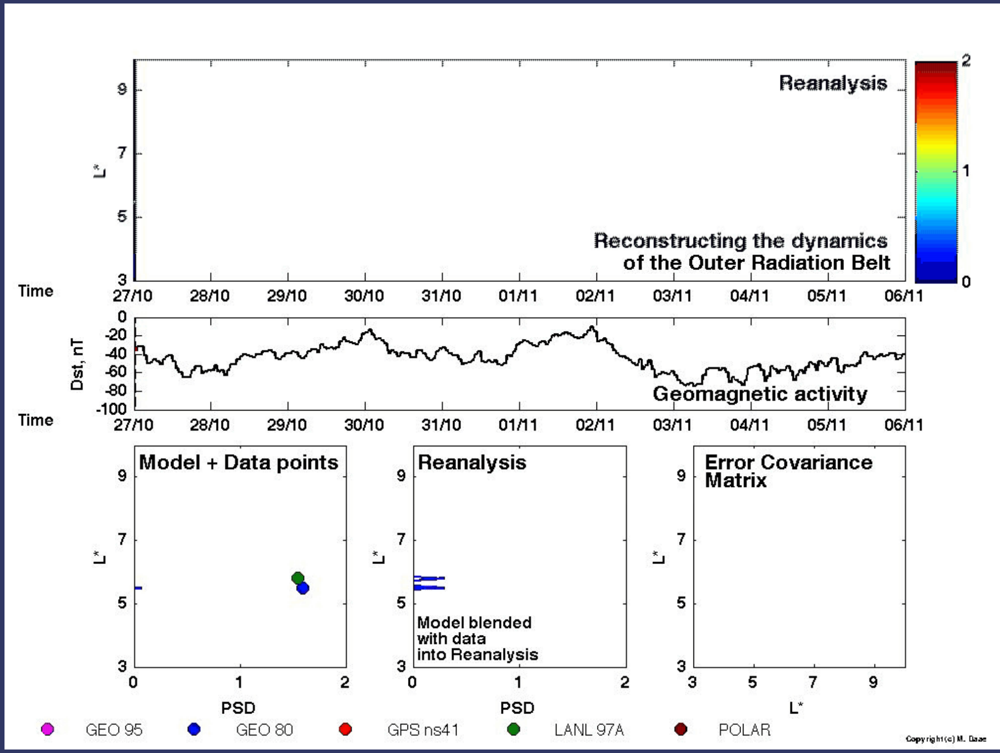

Data is blended with the model according to the underlying structure of data and model errors.

Data from 4 spacecraft is assimilated and radial profile of PSD is dynamically reconstructed

Provided by Marianne Daae

Acceleration of electrons to relativistic energies

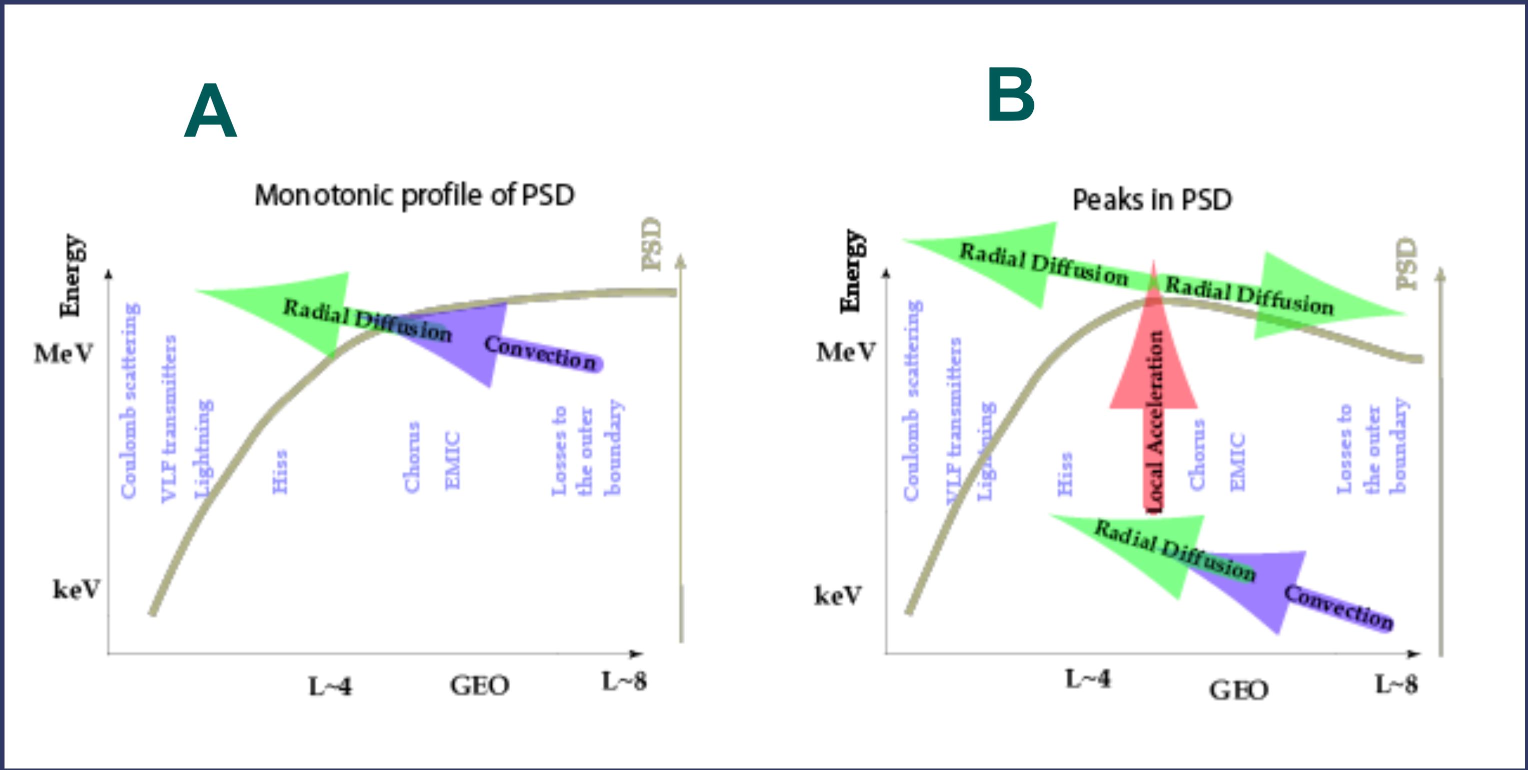

Storm Time Acceleration Mechanisms

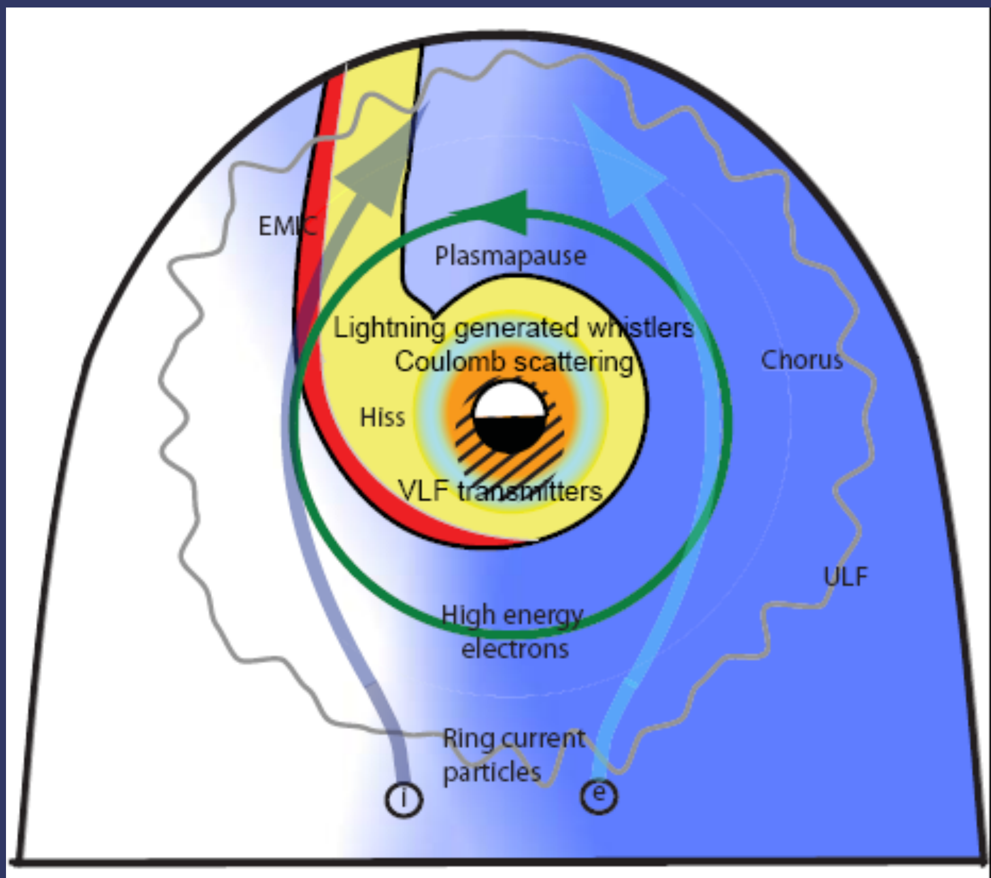

- Inward radial diffusion driven by ULF magnetic field.
- Energy diffusion due to resonance interactions with whistler mode chorus waves
- Shock induced acceleration
- Adiabatic acceleration

Resonant Wave particle interactions

$$\omega - k_{||}v_{||} = n\Omega_e / \gamma, \qquad n = 0, \pm 1, 2, 3, \quad \ldots$$

$$\gamma = (1 - v^2 / c^2)^{-1/2}$$

where ω is the wave frequency, $k_{||}$ and $v_{||}$ are the components of the wave vector and electron velocity parallel to the ambient magnetic field, respectively, Ω_e is the electron gyrofrequency

Resonant interactions occur when multiples of gyrofrequency equal the wave frequency

During resonant interactions, ELF and VLF waves can violate the first and second adiabatic invariants and diffuse electrons in pitch-angle and energy.

$f_{uhr} = \sqrt{(f_{pe}^2 + f_{ce}^2)}$

Dynamical Spectrogram

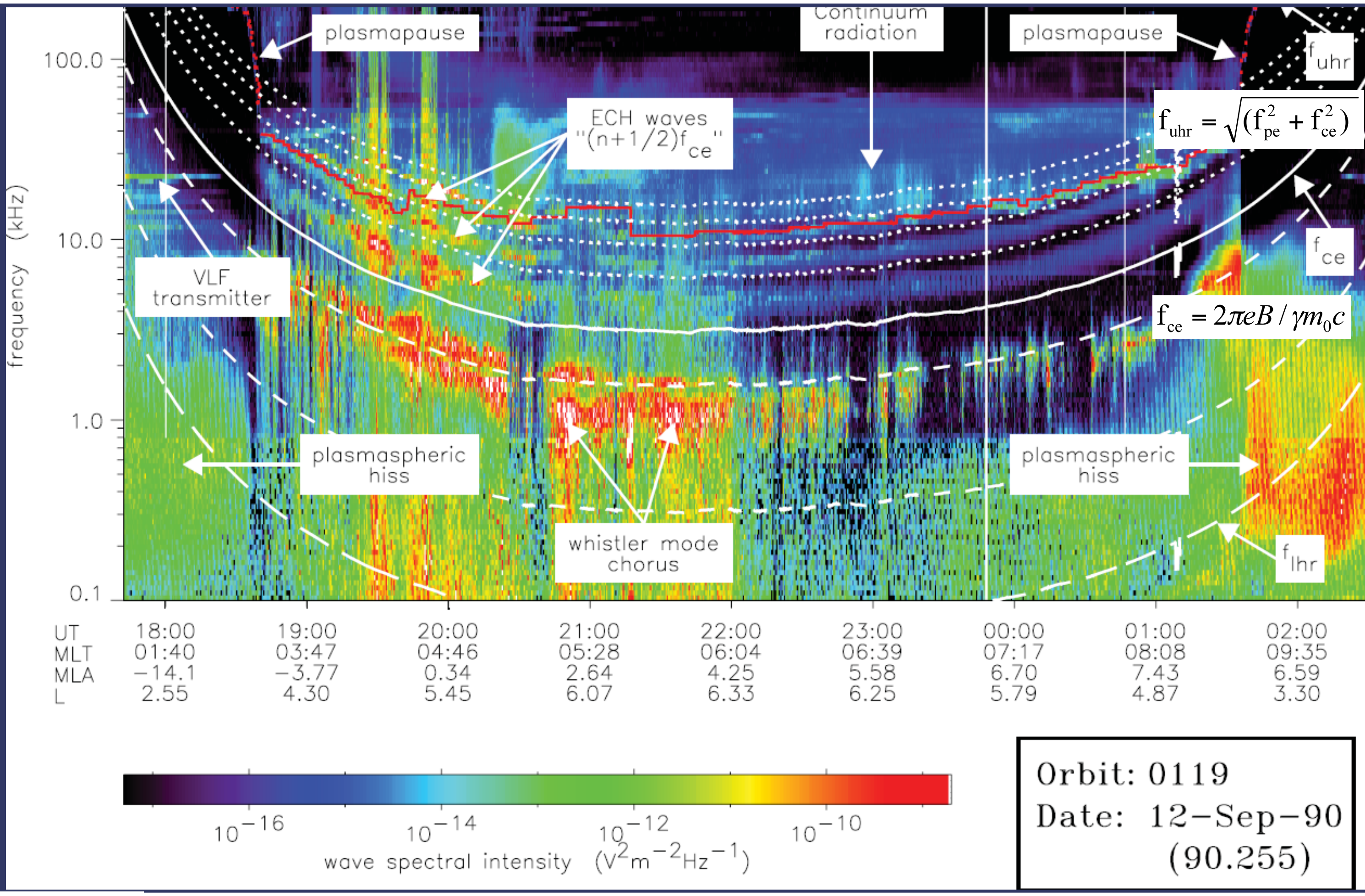

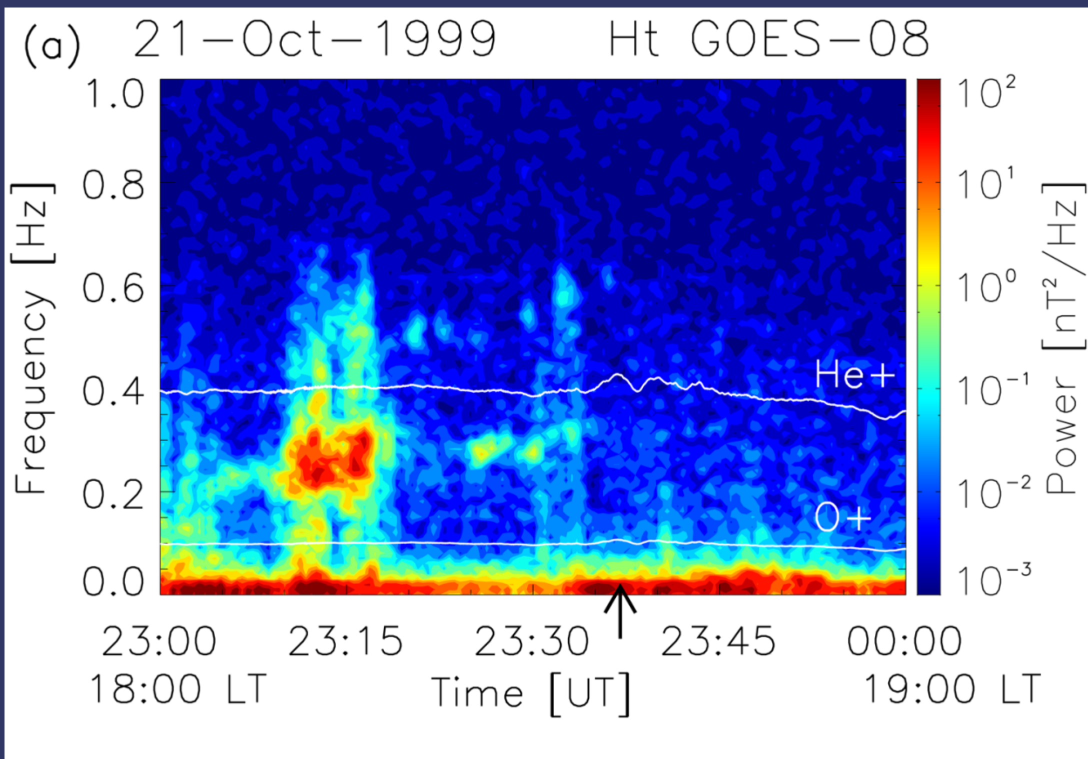

Very intense waves are observed in He band.

EMIC waves can produce scattering of relativistic electrons on very short time scales.

Fraser et al., 2010

Loss of Relativistic electrons in the Radition Belts

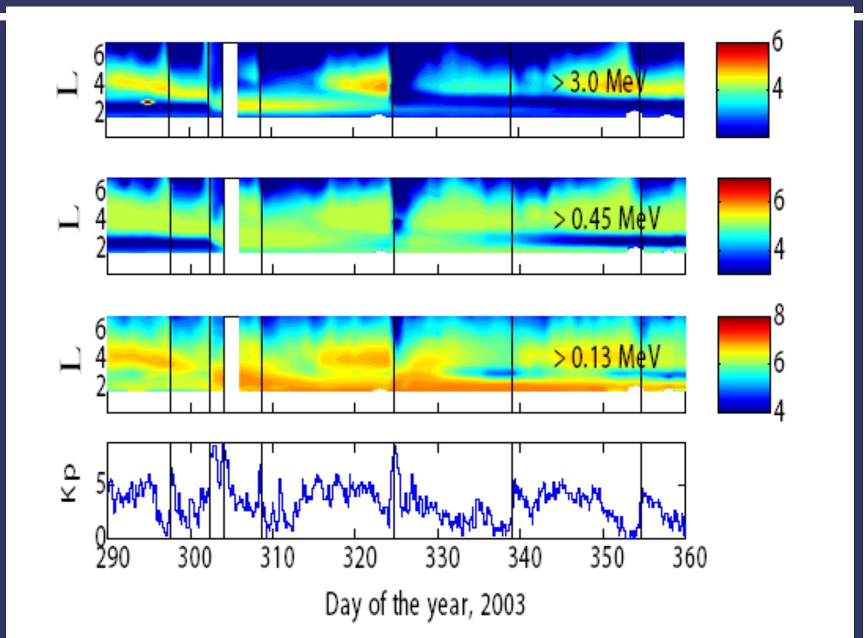

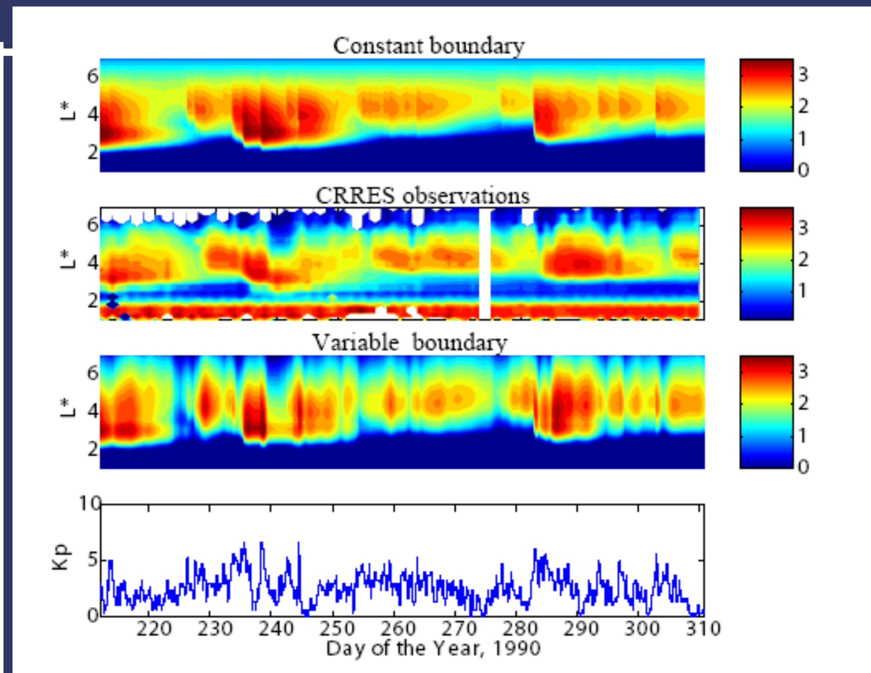

POES Trapped: α = 90 deg at 850 km alt. **POES Precipitating: α = 0 deg at 850 km alt.**

L [R_E]

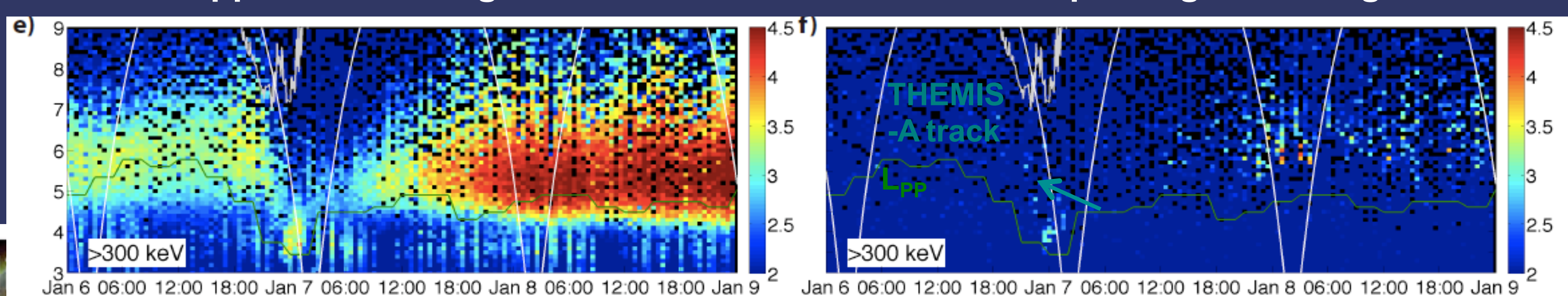

POES Trapped: α = 90 deg at 850 km alt.

POES Precipitating: α = 0 deg at 850 km alt.

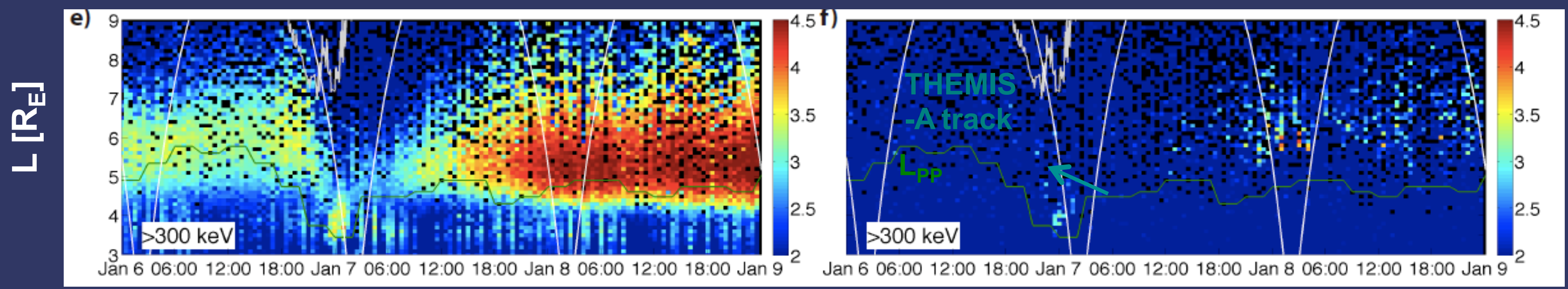

Storm Time Loss Mechanisms

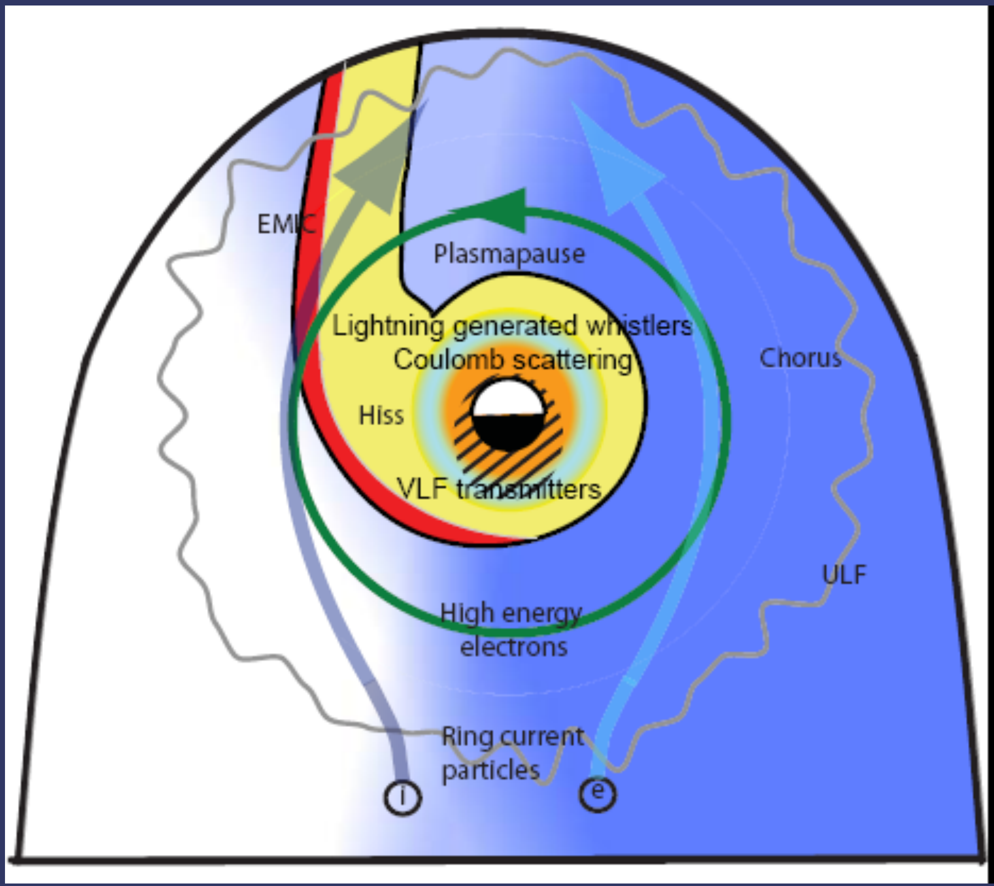

Inward radial diffusion driven by ULF magnetic field.

Energy and Pitch angle scattering due to resonance interactions with different waves

Losses to magnetopause and outward radial diffusion.

Local and Bounce Average Diffusion Coefficnets

$\omega - k_{||} v_{||} = n\Omega_{gyro}/\gamma.$

Local Diffusion Rates

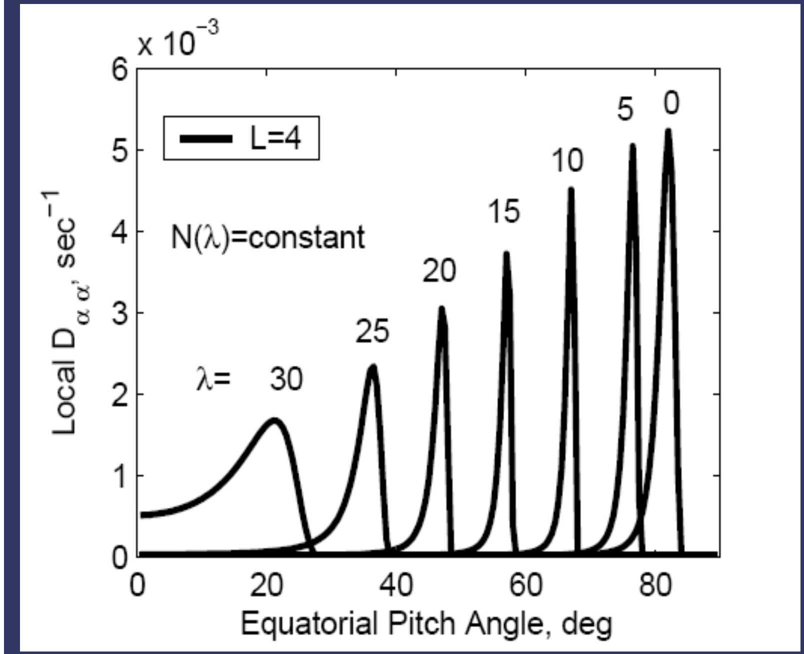

Bounce Averaged Diffusion Rates

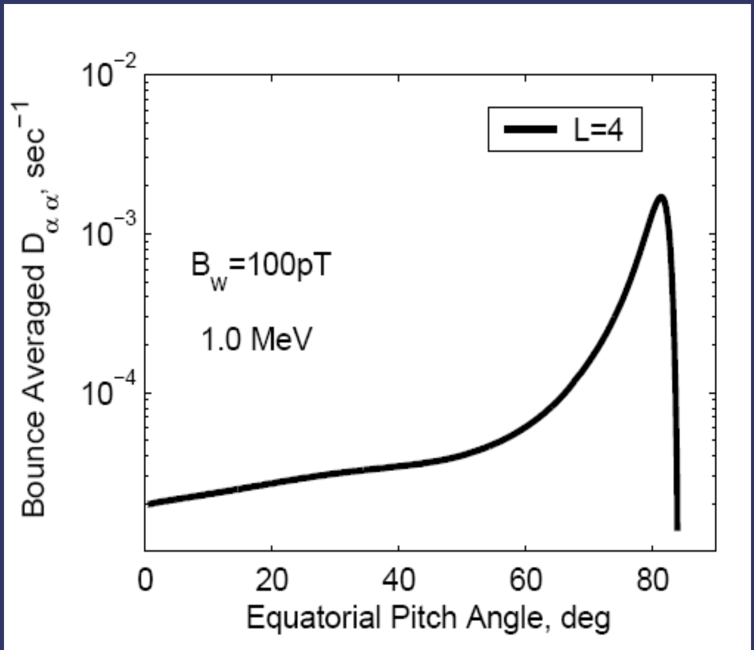

Pitch-angle and energy diffusion coefficients due to resonant wave-particle interactions

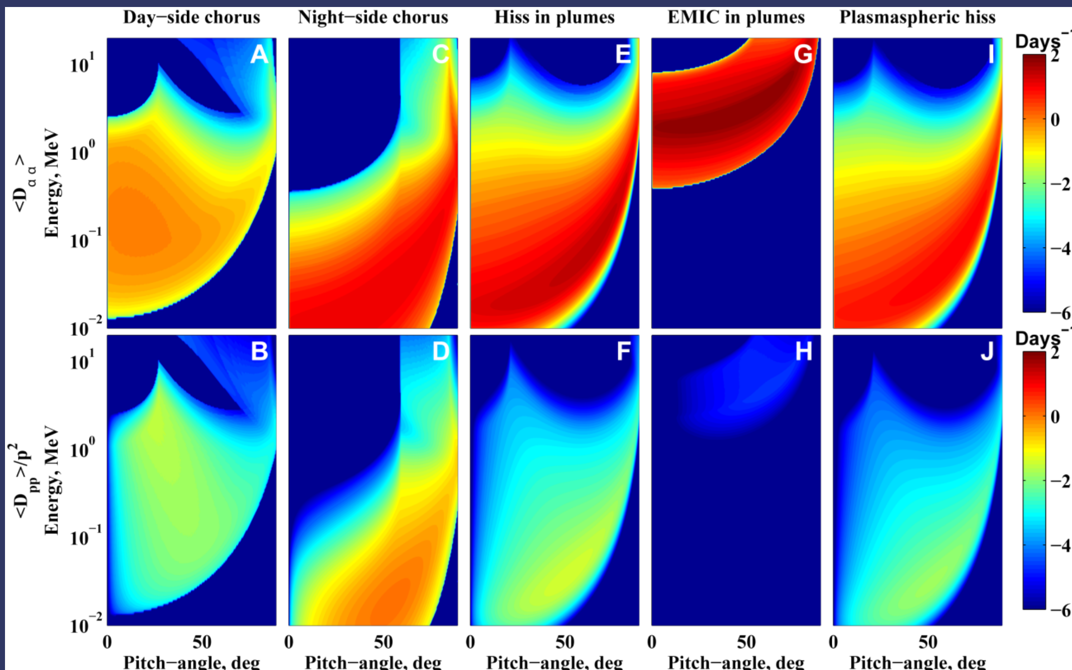

Diffusion rates as due to resonance wave particle interactions with various plasma waves.

Pitch-angle diffusion results in a loss to the atmosphere

Energy diffusion can accelerate electrons locally

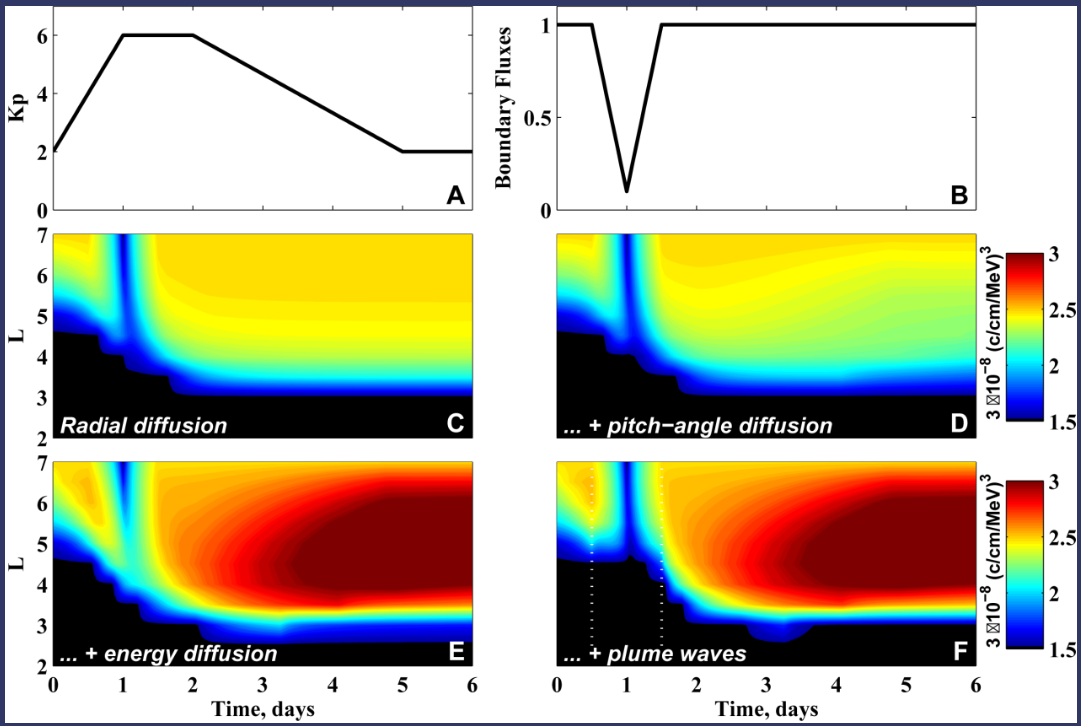

Kp
A
Boundary Fluxes
B
Radial diffusion
C
... + pitch−angle diffusion
D
... + energy diffusion
E
... + plume waves
F
L
Time, days
3 ×10⁻⁸ (c/cm/MeV)³

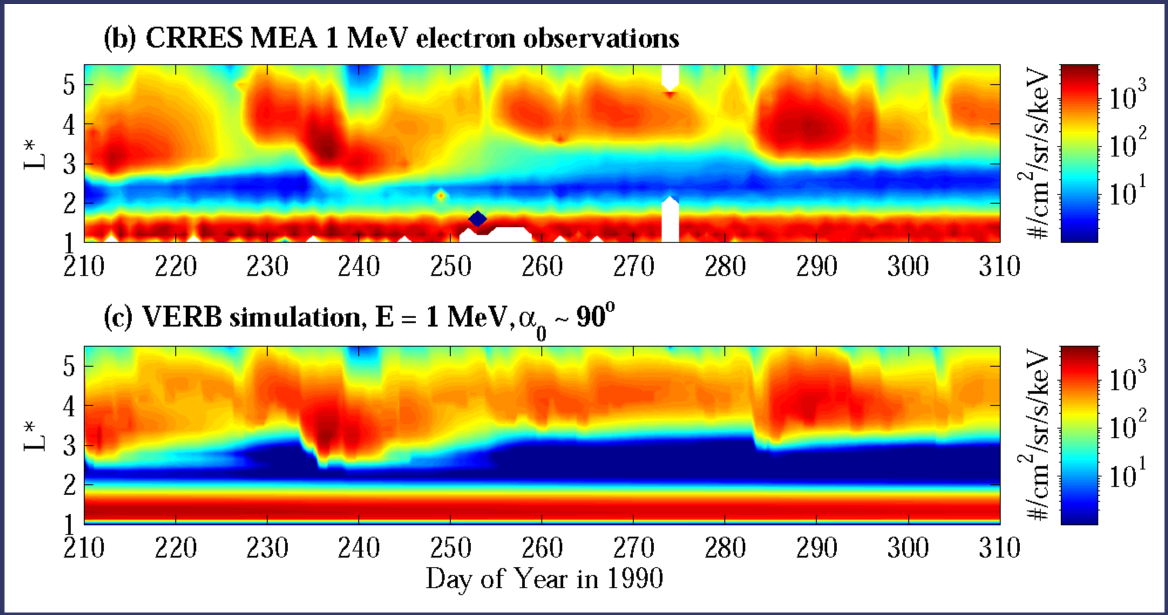

- VERB predicts the instantaneous location of the upper boundary of the slot region, the empty slot region, the stable inner belts, the location of peak of fluxes and amplitude of fluxes.

Proton Radiation Belt: Acceleration Mechanisms

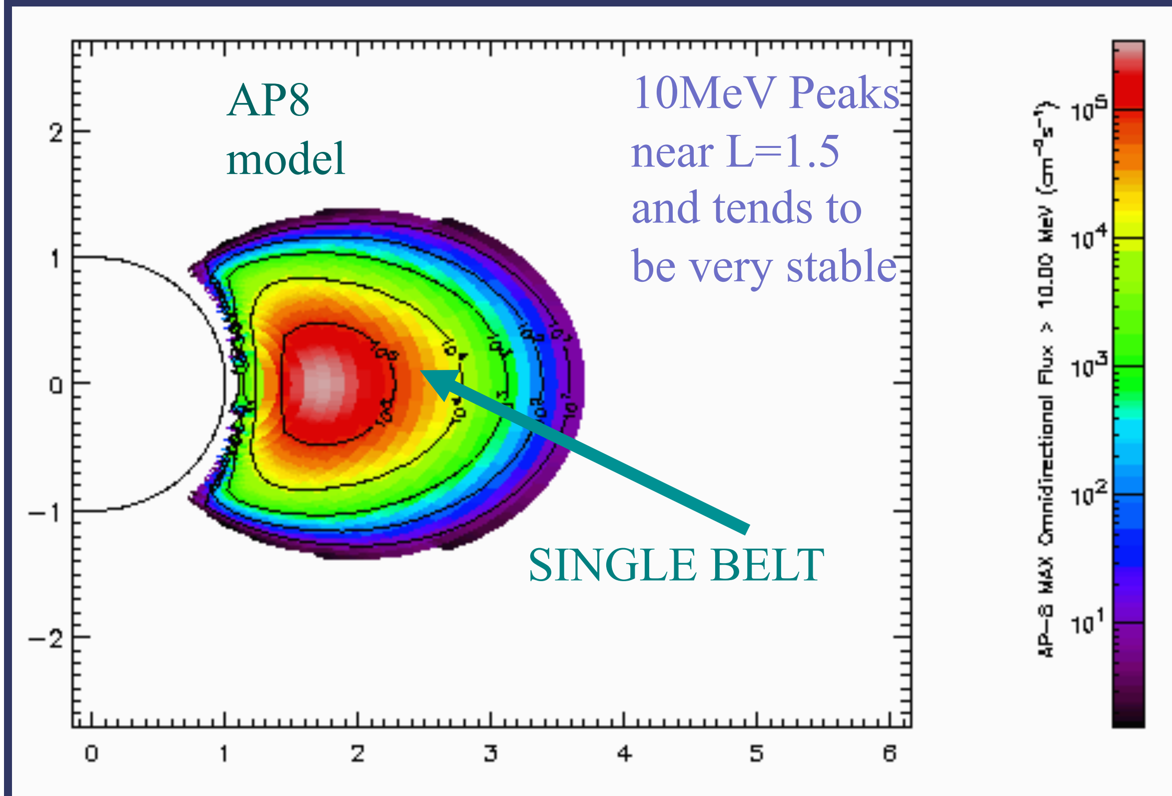

Higher energies peak at lower L-shells

Protons are transported inwards by the large induced electric fields that arise as a large shock passes the Earth.

Can be also transported inwards by radial diffuison

Proton Radiation Belt: Loss Mechanisms

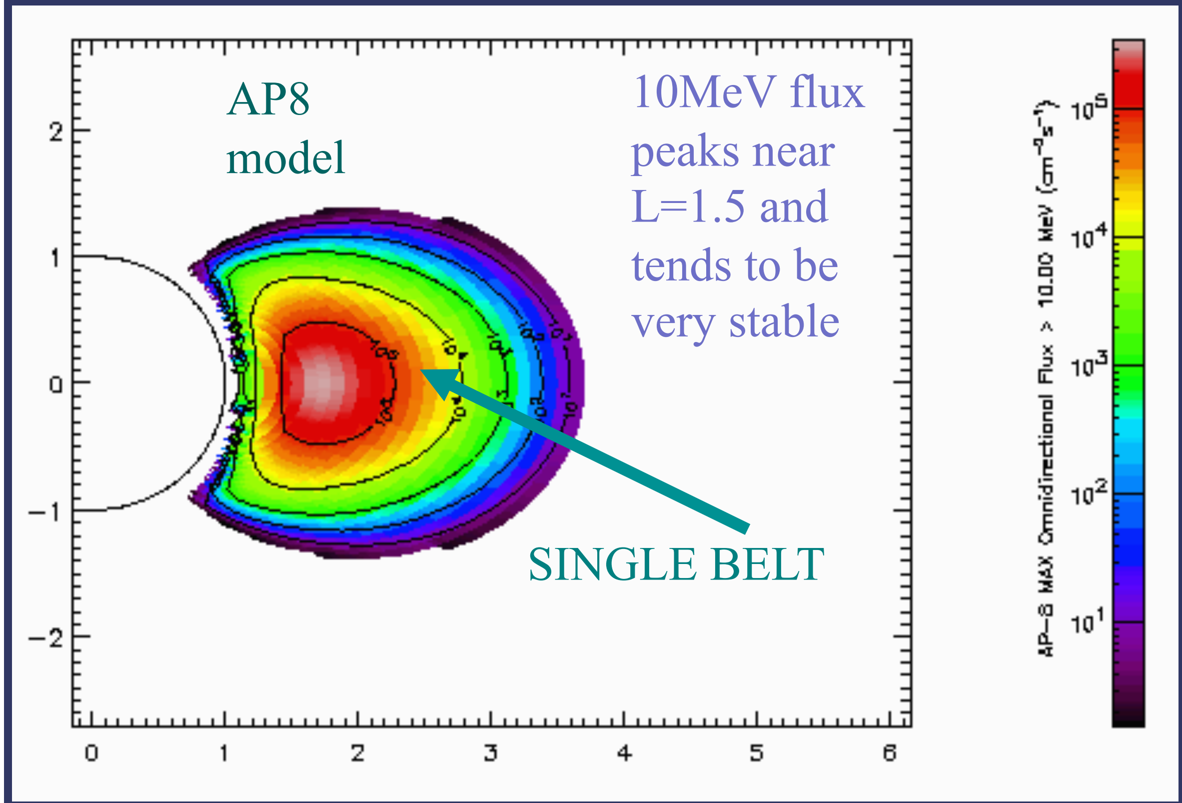

Scattering by EMIC waves

Field line curvature scattering

Adiabatic changes in the inner belt.

Radiation Belts on Jupiter

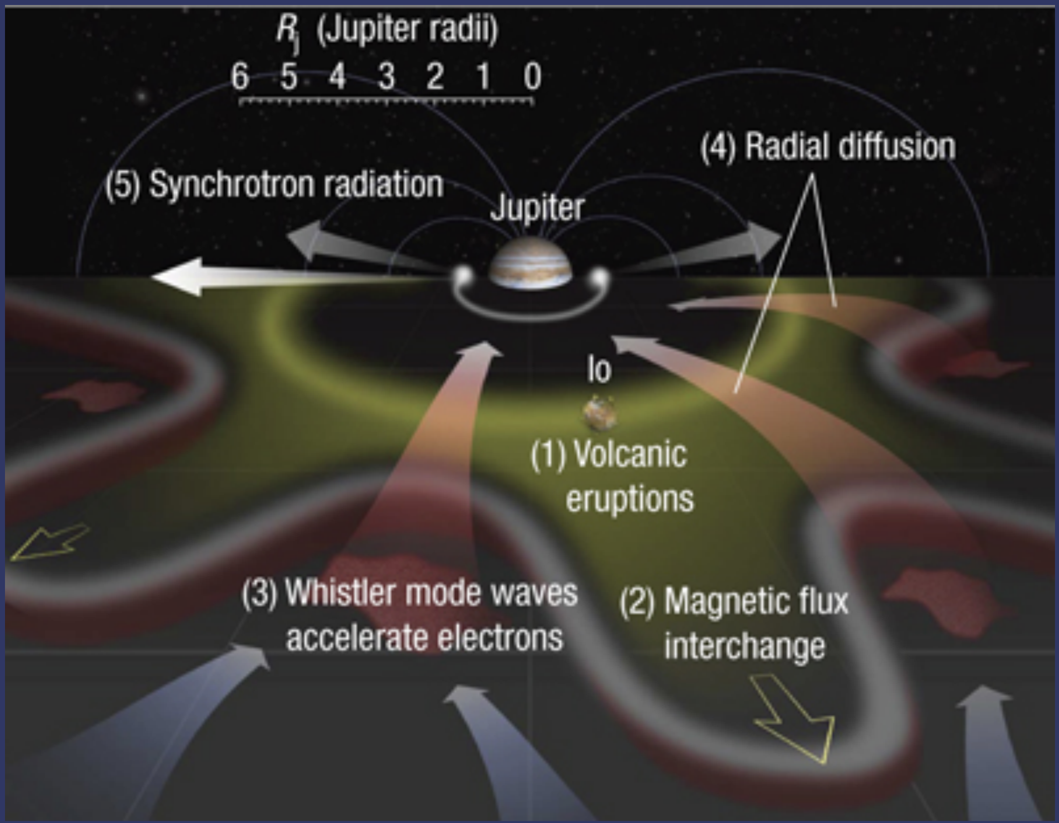

Inward radial diffusion, interchange instability, and energy diffusion chorus waves accelerate elecrons to ultra-relativistic energies.

Losses :interactions with dusty plasmas, planets, synchrotron loss and atmospheric loss.

Horne et al., 2008

Acceleration and Loss of Radiatino Belts on Jupiter

(1) Volcanic gases from Io are ionized and form a cold dense plasma torus around Jupiter.

(2) Jupiter's rapid rotation drives magnetic flux interchange and excites whistler-mode waves.

(3) Gyro-resonant wave–particle interactions accelerate electrons to relativistic energies.

(4) Radial diffusion transports electrons towards the planet and accelerates them to even higher energies via betatron and Fermi processes.

(5) Intense synchrotron radiation is emitted from ultra-relativistic electrons close to the planet ($1.4R_j$).

Particle Trajectories of Ring Current and Radiation Belt Particles

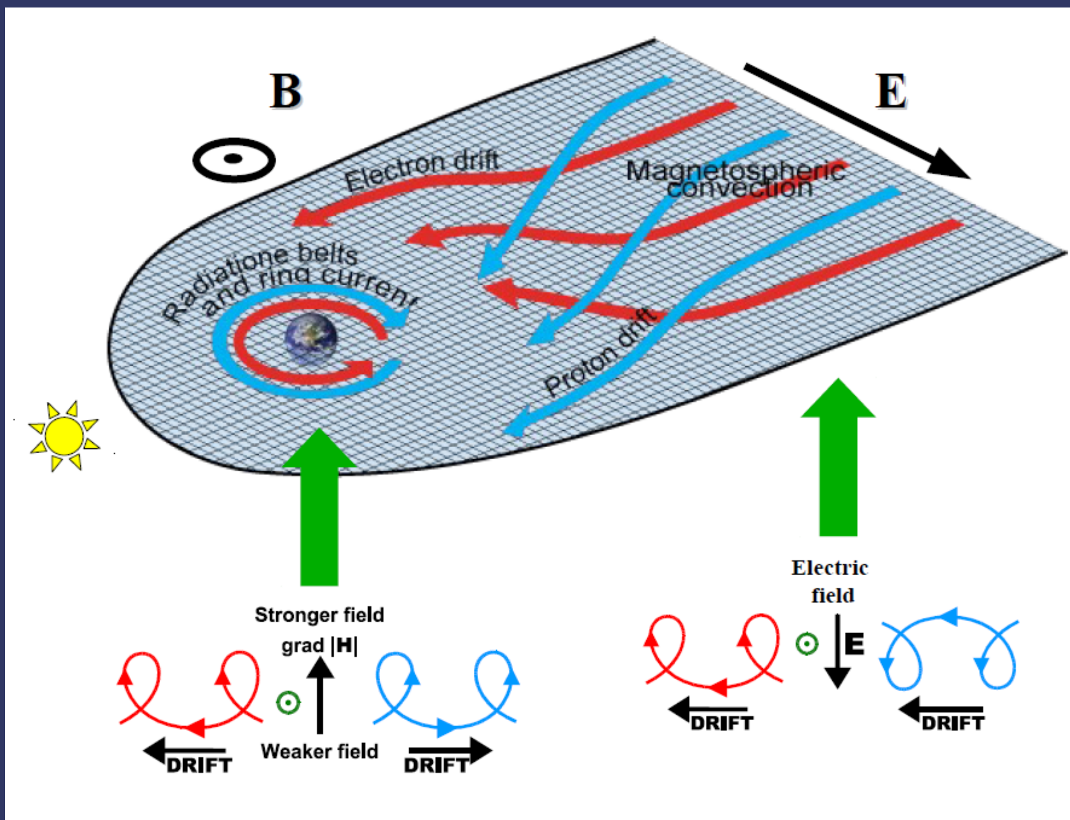

Drift of lower energy particles is dominated by ExB drift.

Radiation Belt particles are subject to the gradient and curvature drifts and will drift around the Earth.

Electrons –eastward,

Ions-westward.

Subbotin, et al., 2011